

Chapter 12

Overview: Imaging in the Study of Integrins

Christopher V. Carman

Abstract

Integrins play critical adhesion and signaling roles during development, wound healing, immunity, and cancer. Central to their function is a unique ability to dynamically modulate their adhesiveness and signaling properties through changes in conformation, both homo- and heterotypic protein–protein interactions and cellular distribution. Genetic, biochemical and structural studies have been instrumental in uncovering overall functions, describing ligand and regulatory protein interactions and elucidating the molecular architecture of integrins. However, such approaches alone are inadequate to describe how dynamic integrin behaviors are orchestrated in intact cells. To fill this void, a wide array of distinct light microscopy (largely fluorescence-based) imaging approaches have been developed and employed. Various microscopy technologies, including wide-field, optical sectioning (laser-scanning confocal, spinning-disk confocal, and multiphoton), TIRF and range of novel “Super-Resolution” techniques have been used in combination with diverse imaging modalities (such as IRM, FRET, FRAP, CALI, and fluorescence speckle imaging) to address distinct aspects of integrin function and regulation. This chapter provides an overview of these imaging approaches and how they have advanced our understanding of integrins.

Key words: Integrin, Fluorescence, Microscopy, FRET, GFP, Conformation, Clustering, migration, Adhesion

1. Introduction

1.1. *The Integrin Family of Adhesion Receptors*

Integrins represent a large family of heterodimeric adhesion/signaling receptors composed of α and β subunits. In vertebrates, 18 α -subunits, and 8 β -subunits form 24 known ab pairs. These exhibit diverse cell expression patterns, ligand-binding properties, and coupling to cytoskeleton and signaling pathways (1). In this way, integrins mediate dynamic cell–cell, cell–extracellular matrix and cell–pathogen interactions and are critical for development, cell migration, phagocytosis, platelet adhesion, and immunological synapse formation.

1.2. Integrin Structure

Both integrin α and β subunits are type I transmembrane (TM) glycoproteins with large extracellular domains, single spanning TM domains and (with the exception of $\beta 4$) short cytoplasmic domains (Fig. 1a). The overall topology of integrins, initially elucidated by electron microscopy studies, revealed a globular N-terminal ligand binding “head” domain (a critical α and β subunit interface) standing on two long C-terminal “legs” or “stalks,” which connect to the transmembrane and cytoplasmic domains of each subunit (2) (Fig. 1a, right). X-ray crystallographic studies have revealed complex domain structure in the extracellular region of both subunits (3, 4). Moreover, such studies demonstrated a surprisingly compact three-dimensional overall topology consisting of legs that were severely bent at the so-called genu or knee generating a V-shaped conformation; In this structure, the head domain was closely juxtaposed to the membrane-proximal portions of the legs, which themselves were in close contact with each other (Fig. 1a, left) (3, 4). As discussed below, the significant differences between early EM and crystallographic studies suggested that integrins possess a propensity for dramatic conformational rearrangements.

1.3. Integrin Dynamics and Regulation

Among adhesion molecules, integrins are unique in their ability to dynamically regulate their adhesiveness through a process termed inside-out signaling or “priming,” which in turn leads to ligand binding and signal transduction in the classical outside-in direction (5). As illustrated in Fig. 1, integrins display a wide array of interdependent dynamics (including changes in conformation, diverse protein–protein interactions, and cellular distribution) that collectively determine their adhesion and signaling properties. In terms of adhesion, the overall strength of cellular adhesiveness (i.e., “avidity”) is governed by (1) the intrinsic *affinity* of the individual receptor–ligand bonds and (2) the number of receptor–ligand bonds formed (*valency*) (5). Whereas, affinity is dynamically modulated by conformational changes in integrins, valency is governed by the

Fig. 1. (continued) mediate diverse protein–protein interaction that include a wide variety of ligands (*left*), cytoplasmic cytoskeletal/signaling molecules (*center*) and membrane proteins (e.g., IAP, uPAR, or tetraspanins) (*right*) proteins. (d) Cellular Redistribution. At a cellular level, integrins dramatically alter their distribution during adhesion and migration over ligand-bearing substrates. On the *left*, a cell is shown with even cell surface distribution. In the *center* is shown a cell spreading on a substrate bearing integrin ligands. Integrins accumulate at an increased density at the substrate interface. On the *right* is shown a polarized migrating cell in which integrins are particularly enriched behind the lead edge of migration. Additionally, intracellular vesicular trafficking of integrins is shown transporting integrins from the trailing to the leading edge. Integrin redistribution, can occur proactively, through the cytoskeleton or vesicular trafficking and/or via mass-action/diffusion. In turn, these properties are strongly influenced by affinity for ligand, microclustering, and cytoskeletal associations.

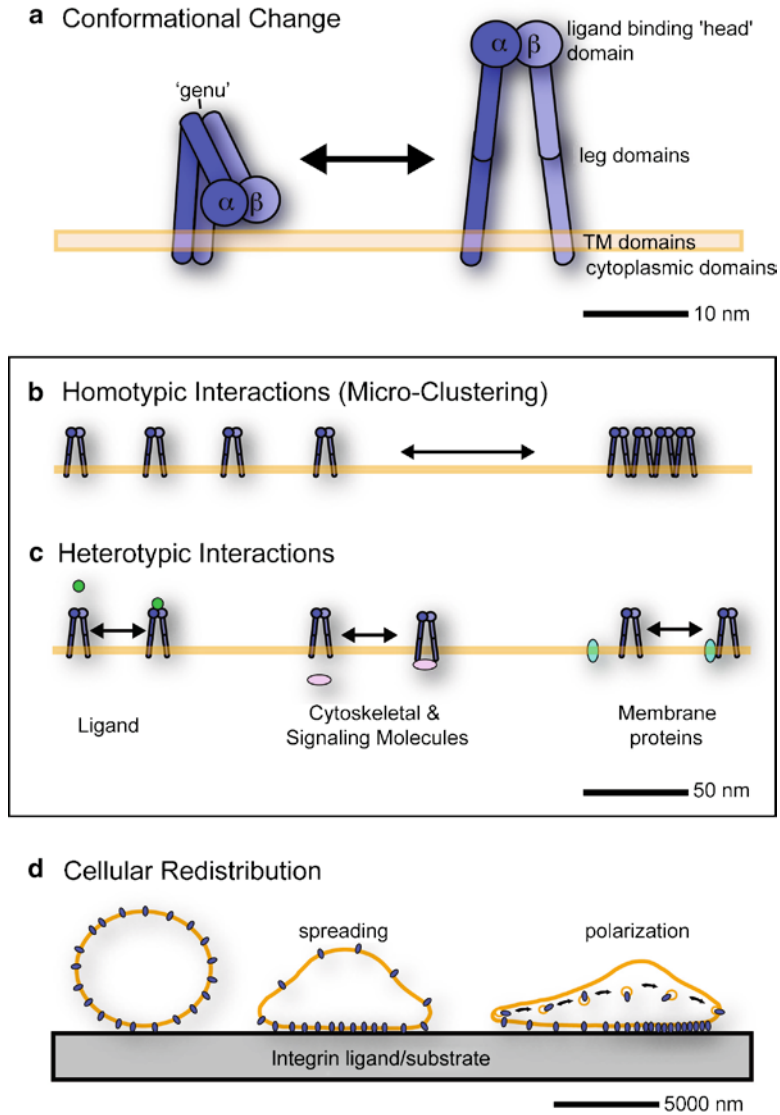


Fig. 1. Integrin Dynamics. Integrin regulation involves interdependent dynamic behaviors that are relevant at a range of spatial scales. (a) Conformational Change. At the molecular level, integrins undergo dramatic large-scale conformational changes, which are coupled to altered affinity for ligand, cytoskeletal proteins, and signaling molecules. The compact “V”-shaped low affinity/inactive conformer (“closed”) is shown on the left. Note the extreme bend in the legs at the “genu,” that the head domain is juxtaposed to the plasma membrane and that the α and β subunit membrane and cytoplasmic domains are closely associated. On the right is the extended (“open”), high-affinity conformer. Note that the head domain sits ~15–20 nm above the plasma membrane and that the membrane and cytoplasmic domains of the α and β subunit have separated. (b) Homotypic Interactions (Microclustering). Integrins undergo lateral associations with each other, which may be driven by direct interaction between individual integrin heterodimers, but also influenced by other protein interactions (see c, below) or association with membrane domains (e.g., lipid rafts). Such micron-scale clustering critically influences adhesiveness and signaling properties. (c) Heterotypic Interactions. Integrins

density of receptor and ligand within the zone of cell adhesion, which in turn is a function of microclustering, diffusion and active transport of integrins, as well as cell spreading (5). Outside-in signaling by integrins is governed by all of the above activities, which also feeds back to modulate these activities (6–10). Thus, a central challenge to understanding integrin function is elucidating how their diverse regulatory processes are integrated.

1.3.1. Conformational change and Affinity Modulation

Studies with soluble monomeric ligands demonstrate that ligand-binding affinity is dynamically modulated in integrins. In resting conditions integrins reside in an inactive state, which exhibits relatively low affinity for ligand. Upon cellular stimulation (e.g., by chemokine) inside-out signaling drives transition to activated states (i.e., with intermediate or high affinity for ligand). It is now known that the “V”-shaped bent (“closed”) integrin conformation (Fig. 1a, left) represents the inactive state, whereas priming and ligand binding are associated with large-scale conformational rearrangements in which the integrin extends (with “switch-blade” like motion) into an “open” conformation (Fig. 1a, right) (11–14). Progressively detailed studies have elucidated mechanisms for linking these global rearrangements to the specific intradomain conformational changes that are directly responsible for affinity modulation (1). In addition to crystallographic, EM and biochemical studies, imaging approaches have been critical for elucidating these mechanisms, as discussed below.

1.3.2. Homotypic Protein Interactions (Microclustering)

Among the mechanisms for regulating avidity (as well as outside-in signaling) formation of laterally associated, micron-scale integrin aggregates (a process termed “microclustering”) is thought to play central roles (Fig. 1b). Several studies suggest that, upon transition to the open conformation, direct homotypic associations between the transmembrane domains of neighboring integrins may be important for driving microclustering (15–18). These interactions may be modulated by association with the cytoskeleton (5, 7, 19–23) and/or association with lipid raft domains (24–27).

1.3.3. Heterotypic Protein Interactions

Integrins undergo dynamic heterotypic interactions with diverse proteins including extracellular ligand, membrane proteins (e.g., tetraspanins, IAP (CD47), uPAR (CD87), and Fcγ receptors (28, 29)), cytoskeletal adaptor proteins and signaling molecules (see Fig. 1c). These dynamics participate in both inside-out signaling/priming (to facilitate adhesion) and outside-in signals (that result from ligand binding) in interdependent ways. For example, binding of multivalent ligands can both be facilitated by integrin microclustering and help drive/stabilize microclusters. Lateral association with tetraspanin membrane proteins may further facilitate integrin microclustering (28). Furthermore, binding and unbinding of cytoskeletal adaptor proteins (e.g., talin, vinculin, paxillin, tensin) also functions both in promoting adhesion and in cellular responses

to ligand binding (5, 7, 19–23). Finally, outside-in signaling responses in integrins are initiated by binding of cytoplasmic signaling molecules, such as FAK, ADAP, ILK, and RapL, as a consequence of both microclustering and ligand-stabilized conformational changes (30–34).

1.3.4. Cellular Redistribution

In addition to microclustering (discussed above), integrins dramatically modulate their cell surface distribution on a broader scale, particularly during processes of spreading, polarization, and migration on adhesive substrates and during phagocytosis and immunological synapse formation (32, 35–37) (Fig. 1d). Studies have shown dynamic changes in tethering to the cytoskeleton during activation and ligand binding alter integrin diffusivity and, thus, the propensity to redistribute to or from zones of contact with ligand (5, 7, 19–23, 38). In addition, active processes, such as vesicular trafficking of integrins (39, 40) and Rap1- and RapL-driven polarization of integrins to the lamellipodia (41, 42), represent important active modes of integrin redistribution (Fig. 1d).

2. Light Microscopy in the Study of Integrins

The previous section illustrates that integrin function/regulation involves a variety of discrete, yet interdependent, dynamics, each with distinct spatial and temporal scales. Thus, understanding integrin function/regulation requires a range of approaches suitable to the investigation of each of these dynamics. Though imaging through electron and scanning probe (e.g., atomic force) microscopy have utility in studying integrins, optical/light microscopy-based imaging (especially using fluorescence) has proven to be exceptionally powerful in this regard and is the focus of this chapter.

“Light microscopy” comprises an increasingly complex collection of approaches that can provide diverse types of information when applied to biological samples. Fundamentally, these approaches derive from the combination of specific microscope system designs (referred to here as “microscope technologies”) and methods of using these systems (i.e., “imaging modalities”). In the following sections we will describe fundamental aspects of the major light microscope technologies and imaging modalities along with discussion how each have been applied to the study of integrins.

2.1. Nonfluorescence Light Microscopy

In its simplest form, light microscopy involves shining white light on a sample and using lenses to variously assess the light transmission, reflection, and diffraction as it interacts with the sample. Commonly used optical configurations include bright field, phase contrast and differential interference contrast (DIC), which are all broadly applicable to visualizing cells (43). In the context of integrin substrates, these techniques provide important, albeit

indirect, measures of integrin function by allowing visualization of cell adhesion, spreading, polarization, and migration.

Interference reflection contrast microscopy (IRM) is a somewhat more specialized imaging technique, which is particularly well-suited for characterizing aspects integrin function. The basic principal of IRM is the imaging of interference patterns in reflected light created by thin (on the order of a fraction of the wavelength of light) spaces between materials, such as those between a coverslip and an opposing cell membrane (44). Several relatively simple optical configurations can be used to achieve IRM imaging on basic light, as well as laser-scanning confocal (see below), microscopes (44–46). IRM is particularly useful for imaging the distribution and dynamics of areas of cell–substrate adhesion where the close apposition gives rise to dark areas against a bright background of reflected light. Such dark spots are often correlated with clusters of integrins and integrin-associated proteins (e.g., vinculin and talin) marking specific adhesion structures, such as focal contacts, focal adhesions, podosomes, invadopodia and immunological synapses (37, 44–47).

Finally, single particle tracking (SPT) is a nonfluorescent method for direct visualization of diffusive dynamics of individual integrin molecules on the membrane surface (48). SPT uses optically dense ($\sim 1 \mu\text{m}$) polystyrene beads coated with low density of antibody or ligand, which serve as probes for membrane proteins (48). When coupled to DIC imaging at high temporal resolution, SPT can extract information on the trajectory of integrin movement and diffusion coefficients (48). In this way, SPT has shown that the diffusion of the integrin LFA-1 is determined by both integrin conformation and cell activation status and that confinement of LFA-1 by cytoskeletal attachment regulates cell adhesion both negatively and positively (20, 21, 38).

2.2. Fluorescence Light Microscopy

By far the most broadly used imaging approaches to characterize the distribution dynamics and activity of integrins in intact cells and tissues are those based on fluorescence microscopy. Through use of appropriate tags/probes (see below) that label integrins (or related molecules of interest) fluorescence microscopy allows dynamic and noninvasive molecular imaging. As discussed in this section, these fundamental techniques offer flexible building blocks for diversely informative imaging modalities.

2.2.1. Fluorescence Defined

Fluorescent molecules (i.e., “fluorophores” or “fluorochromes”) exhibit the property of being able to “borrow” photons of light for short periods of time before releasing them at a lower energy level (i.e., of a longer wavelength) (Table 1 and Fig. 2a–c). Ideal fluorophores exhibit a sharply defined wavelength range that they can absorb (i.e., excitation/absorption maxima). Upon photon absorption fluorophore electrons are raised to an excited state. After resonating for a period of time (“fluorescence lifetime”;

Table 1
Fluorescence terminology

Term	Definition/comments
Absorption	The uptake of an incident photon by a fluorophore, which drives its electrons into an excited state
Auto-fluorescence	Endogenous fluorescence within a sample that may provide significant background “noise,” particularly when using higher energy excitation (i.e., shorter wavelengths). In cells auto-fluorescence mostly comes from pyridinic (NADPH) and flavin coenzymes, as well as aromatic amino acids and lipo-pigments. Unhealthy/dyeing cells exhibit elevated auto-fluorescence. In tissues, extracellular matrix proteins (e.g., collagen and elastin) provide a significant source of auto-fluorescence
Brightness	The overall intensity of a fluorophore defined by its extinction coefficient, quantum yield, and photo-stability
Contrast	The degree to which specific fluorescence can be distinguished from reflected light and auto-fluorescence. Contrast is determined by fluorophore brightness and concentration, as well as, imaging parameters, such as intensity of excitation light source and exposure time
Emission	Photon release from an excited fluorophore during relaxation to the ground state
Emission maxima	The center point in a distribution curve of light wavelengths that are most intensely emitted by a specific fluorophore after excitation
Excitation	The elevation of a fluorophore to an excited electronic state as a result of absorbing a photon
Excitation Maxima	The center point in a distribution curve of wavelengths that are most efficiently absorbed by a fluorophore
Extinction coefficient	A measurement of how strongly a chemical species absorbs light at a given wavelength
Fluorochrome	See fluorophore
Fluorophore	A component of a molecule, which causes a molecule to be fluorescent. The amount and wavelength of the absorbed and emitted energy depend on both the fluorophore and the chemical environment of the fluorophore
Fluorescence	The process of by which certain molecules (i.e., fluorophores) absorb photons of a specific wavelength, become electronically “excited” and then “relax” to the ground state by emitting a photon of reduced energy (and longer wavelength)
Fluorescence lifetime	The average time the molecule stays in its excited state before emitting a photon
Photo-activation	The property of certain fluorophores to require absorption of specific wavelengths of light in order to produce photo-chemical conversion from a nonfluorescent to a fluorescent state
Photo-bleach	The photo-chemical destruction of a fluorophore as a result of photon absorption

(continued)

Table 1
(continued)

Term	Definition/comments
Photo-switching	The property of certain fluorophores to undergo photo-chemical conversions that alter their fluorescent properties (specifically absorption and emission maxima) as a consequence of photon absorption
Photo-stability	The relative resistance of a fluorophore to photo-bleaching
Photo-toxicity	A phenomenon known in live-cell imaging in which illumination of a fluorophore causes the cell damage and death. The main cause for photo-toxicity is the formation of oxygen radicals due to nonradiative energy transfer
Stokes shift	The difference between absorption and emission maxima for a given fluorophore
Quantum yield	The efficiency of the fluorescence process, defined as the ratio of the number of photons emitted to the number of photons absorbed
Quenching	Any process which decreases the fluorescence intensity of a given substance. A variety of processes can result in quenching, such as excited state reactions, energy transfer, complex-formation, and collisional quenching

typically on the scale of nanoseconds), the fluorophore electrons “relax” back to the ground state, releasing a photon in the process (“emission”). Emitted photons are of lower energy and, therefore, of longer wavelength than the absorbed photons. The difference in excitation and emission wavelengths is known as the Stokes Shift. The commonly used green fluorophores FITC, Alexa488, and GFP absorb blue photons (~490 nm wavelength) optimally and in turn releases lower energy green light (~520 nm) and, thus, have Stokes Shift of ~30 nm (Fig. 2b). The red fluorophores rhodamine, Cy3, and DsRed absorb yellow light (~530 nm) and emit red light (~570 nm; Stokes Shift is ~40 nm) (Fig. 2c). The principal of fluorescence microscopy is to take advantage of the Stokes Shift, using carefully designed wavelength-specific filters (or alternate techniques) to separate reflected excitation light from the emitted light. When fluorophores are used in conjunction with appropriate “probes” (see below) they enable noninvasive and dynamic imaging of molecules of interest in intact cells.

In practice, there are several fundamental features of fluorescence that need to be carefully considered/managed to produce effective imaging (Table 1). Extinction coefficient, quantum yield, photo-stability/photo-bleaching and photo-toxicity are among the most critical. Extinction coefficient describes the efficiency of photon absorption by a fluorophore, whereas quantum yield is the efficiency with which excited fluorophores ultimately emit photons. Together these parameters determine brightness. The process of fluorescence is usually coupled to oxidative destruction of the fluorophore

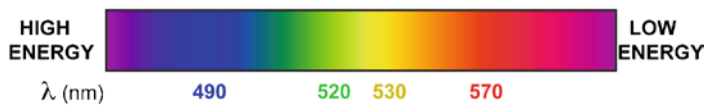
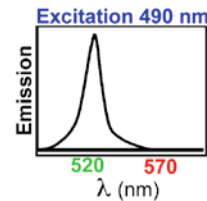
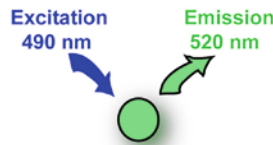
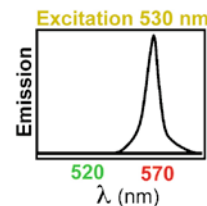
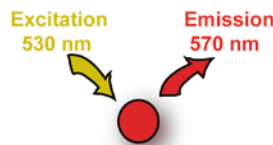
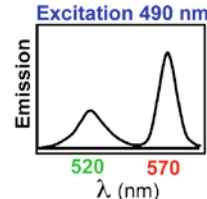
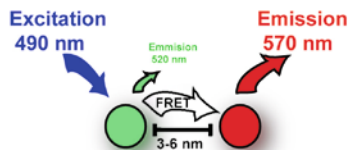
a Visible Light Spectrum**b** Green Fluorescence**c** Red Fluorescence**d** Fluorescence Resonance Energy Transfer (FRET)

Fig. 2. Basics of Fluorescence and FRET. **(a)** Visible light spectrum displaying from left to right high to low energy (i.e., short to long wavelength). **(b, c)** The principle of fluorescence illustrated for two distinct fluorophores, which have properties roughly similar to common green (e.g., FITC, Alexa488, GFP; **b**) and red (e.g., Rhodamine, Cy3, DsRed; **c**) fluorophores. In each case, the emitted photons are shifted toward lower energy/longer wavelengths than those absorbed (i.e., exhibit a Stoke's Shift) due to energy dissipation during excited state "vibrations." **(d)** Fluorescence Resonance Energy Transfer (FRET). FRET is the nonradiative (that is without intermediate emission of a photon) transfer of excited state energy from on "donor" fluorophore to an "acceptor" fluorophore. FRET is a highly distance-dependent phenomenon and can be used as a "spectral ruler" to measure conformational changes or molecular interaction on the spatial scale of $\sim 3\text{--}6$ nm. Thus, when appropriately matched donor and acceptor come into close proximity and are exposed to light close the donor absorption maxima the donor emission becomes quenched and in turn the acceptor fluorophore undergoes "sensitized emission." In practice, FRET assays often monitor donor quenching, sensitized emission or donor fluorescence lifetime as a readout for FRET.

(photo-bleaching). Fluorophores exhibit vastly differing resistance to such destruction (i.e., photo-stability). Oxidative processes (e.g., reactive oxygen species (ROS) generation) that are coupled to absorption of photons both by fluorophores and endogenous "auto-fluorescent" molecules (see Table 1) can produce damage to proteins and other biomolecules that may substantially compromise cell

health (i.e., cause cytotoxicity, a process specifically referred to as “photo-toxicity”). Central challenges in fluorescence microscopy are to manage signal strength, contrast and resolution, while minimizing bleaching and toxicity, which are particularly important for thick samples or those requiring repeated imaging over long durations.

2.2.2. Fluorescent Probes

Meaningful fluorescence microscopy requires specific labeling of biomolecules of interest with appropriate fluorescent molecules (i.e., via “fluorescent probes”). Fluorophores and tagging techniques widely used in the study of integrins are discussed below.

Fluorophores: Commonly used fluorophores can be classified as small (molecular weights ~300–500 kDa) organic dyes, fluorescent proteins (FPs), and quantum dots (QDs). Traditional fluorescein- and rhodamine-based dyes have been broadly used, but recently replaced by a wide spectral variety of new generation Alexa and Cy dyes, which exhibit superior brightness, photo-stability and hydrophilicity. These are available in broad formats for chemical conjugation to molecules of interest. Fluorescent proteins (FP) are ~30 kDa β -barrel domains surrounding a cyclized peptide fluorochrome. Since the discovery of green fluorescent protein (GFP) from the *Aequorea* jellyfish, a full pallet of FP colors have been discovered/engineered (49, 50). In addition, a variety of photo-activatable, photo-switchable, pH-sensitive, and reactive oxygen species (ROS) photo-synthesizing FPs have been developed that support advanced imaging approaches (49, 50). QDs are inorganic nano-crystals of ~10–30 nm in size that exhibit brightness that is ~10–100-fold greater than organic dyes or FPs and are virtually non-photo-bleachable (50).

Techniques to Tag Proteins: Basic approaches for tagging biomolecules of interest include immunolabeling and genetic tagging. Immunolabeling uses antibodies that have been covalently conjugated with either small organic dyes or QDs. Immunolabeling can be accomplished using primary antibodies directly conjugated to fluorophore or by combination of nonfluorescent primary antibody followed by fluorescent secondary antibodies. This indirect approach is widely used for its relative convenience (based on the broad commercial availability of conjugated secondary, but not most primary antibodies), but has limited flexibility for concomitant labeling of multiple proteins (based on the need for primary antibodies derived from distinct species). Whether, using a direct or indirect approach, a further concern relevant to live-cell imaging is the fact that antibodies are relatively large (~150 kDa) and bivalent molecules, which can induce protein cross-linking or otherwise alter target function through steric effects. This can be partially overcome by use of enzymatically generated monovalent antibody fragments (fAbs; ~50 kDa). The large extracellular epitope surfaces of integrins have made them easy targets for immunolabeling. Moreover, their profound

conformational changes associated with activation have been exploited to generate antibodies specific for active conformations. In this way, researchers have been able to concomitantly monitor distribution and activation state.

Genetic tagging involves modifying the sequence of the protein of interest to directly incorporate a fluorescent tag (i.e., FP) or to incorporate a sequence that can facilitate the subsequent labeling with an exogenous fluorescent tag. FPs have become widely used in the study of integrins though fusing them (usually with use of several amino acid flexible linkers) to the C terminus of integrin α - and β -subunits (see Fig. 3). Additionally, many

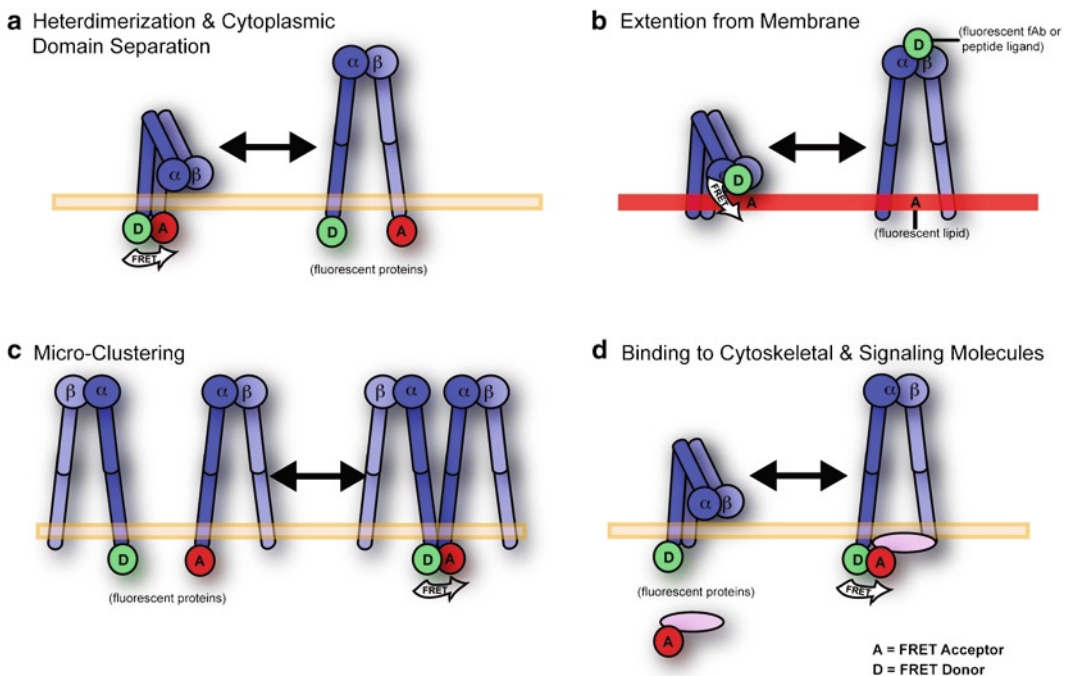


Fig. 3. FRET Approaches to Studying Integrins. FRET has been profoundly important for characterizing integrin regulation and employed in diverse ways to address distinct question. (a) Heterodimerization and Cytoplasmic Domain Separation. Integrin α and β subunits are differentially fused to FPs that can serve as FRET donors (“D”) and acceptors (“A”). Strong FRET under basal conditions demonstrated that the when heterodimers form, α and β cytoplasmic domains are in close apposition. Strong loss of FRET upon integrin activation, ligand binding in the extracellular domain or talin binding in the cytoplasmic domain demonstrated the separation of the cytoplasmic domains in such settings. (b) Head Domain Extension from the Plasma Membrane. Fluorescent fAb fragments or peptide ligands that bind the head domain are used as FRET donors. Fluorescent lipids that intercalate into the plasma membrane are used as acceptors. Strong quenching of donor signal in the basal state that was relieved by activation or ligand binding demonstrated in intact cells that the head domain extends away from the plasma membrane during activation. (c) Microclustering. Similar to A, above, FP donors and acceptors are fused to the cytoplasmic domains. However, here donor and acceptor are both on either the α or the β subunit. In this experimental design significant FRET can only occur if individual heterodimers come into close apposition. (d) Binding of Cytoskeletal and Signaling Molecules. Donor and acceptor FPs are differentially fused to the cytoplasmic domain of one of the integrin subunits and a signaling/cytoskeletal protein of interest in order to monitor integrin binding to cytoplasmic proteins.

integrin-binding proteins such as talin, vinculin, paxillin, and focal-adhesion kinase (FAK) have similarly been labeled with FPs at their N- or C-termini. Thus, distribution dynamics of integrins and integrin interacting proteins can be monitored concomitantly in intact live cells (see Fig. 3).

The concept of indirect genetic tagging was first introduced by the addition of small peptide epitopes (e.g., “Myc,” “Flag,” and “HA” epitopes), to provide reactivity to well-characterized antibodies. This, “engineered” immunolabeling approach suggested potential for more diverse and flexible protein tagging strategies. The first such strategy to be realized involved addition of a 12 residue peptide sequence to intracellular proteins that allows for specific and high-affinity binding of the membrane permeable biarsenical green and red fluorophores “FLAsH” and “ReAsH,” respectively (49). However, several critical technical issues, including the cytotoxicity of the dyes, have severely limited the utility of this approach. Recently, another novel strategy was developed using the integrin LFA-1 and the fungal enzyme cutinase in combination with its suicide substrate p-nitrophenyl phosphonate (51). Thus, cutinase was genetically inserted into the extracellular domain of LFA-1 in a manner that did not appreciably influence integrin function or conformational regulation. In this way, it became possible to efficiently, specifically, and covalently label cell surface LFA-1 integrins with p-nitrophenyl phosphonate-conjugated small molecules and QD fluorophores (51).

Integrin ligands as fluorescent probes. Integrin ligands themselves, as well as integrin small molecule inhibitors, have been employed as integrin imaging probes with unique properties. In the simplest form, small molecule and peptide ligands conjugated to fluorophore have been used in a manner similar to antibodies to label integrins. For example, fluorescein-conjugate derivatives of the LDV tri-peptide VLA-4 ligand or synthetic LFA-1 inhibitor BIRT-377 have both been used as integrin probes to monitor integrin conformation in the context of specific FRET assays (see below) (52, 53). Fluorescent ligands presented in the context of membrane can provide a readout for integrin behavior that is somewhat less direct, but in some ways more physiologic. An excellent example of this is the use of fluorescently conjugated ICAM-1 (a ligand for LFA-1) linked to a membrane tether (GPI) presented on the surface of a glass supported lipid planar bilayer as a readout for integrin rearrangements during formation of immunological synapse (37). With this approach, the initial integrin clustering and ligand binding by lymphocytes at the center of adhesive contacts and the progressive rearrangement into “peripheral supramolecular adhesion clusters” (pSMACs) during antigen recognition were defined (37). Moreover, VCAM-1 (a ligand for the integrin VLA-4)- and ICAM-1-FP fusion proteins transfected into adherent cells (e.g., endothelial, epithelial, or CHO K1)

provides a readout for integrin-driven ligand clustering, membrane reorganization, and topological alterations (including formation of “transmigratory cups,” “docking structures,” podosomes’, and “adhesion rings”) during migration of blood leukocytes (54–58).

2.2.3. Basic Wide-Field Fluorescence Microscopy

Wide-field fluorescence or “epifluorescence” microscopy is perhaps the most versatile, accessible, and affordable approach for conducting fluorescence imaging (see Table 2). Typical epifluorescence systems use a broad-spectrum excitation light source (e.g., mercury or xenon arc lamp) that is directed through an excitation filter to select desired excitation wavelengths (i.e., appropriate for a specific fluorophore in the sample). This light then passes through an objective lens and floods the entire sample imaging field with photons (hence the term wide-field). Reflected incident light and emitted fluorescent light pass back through the objective and then are then filtered by a combination of a dichroic mirror and emission filter (matched to the emission maxima of the fluorophore) before traveling to the detector (typically a charge-coupled device (CCD) camera).

Inherent advantages of wide-field imaging include sensitivity (and therefore the ability to use relatively low intensity excitation) along with relatively rapid image acquisition. Thus, for many (at least in vitro) systems wide-field microscopy is an excellent choice for dynamic imaging. As stated above, such systems are flexible and easily combined with most basic and advanced (e.g., FRET, FRAP, FLIP, etc.) fluorescence imaging modalities. Moreover, it is relatively straightforward to acquire multiple fluorescence and nonfluorescence channels in parallel over time. As a result, this basic technology has been used in an enormous number of studies to concomitantly image the localization dynamics of integrins and integrin-associated proteins during processes such as adhesion, migration, and phagocytosis. As discussed below, the most significant deficiency in wide-field imaging comes in the resolution of submicron range information (particularly when handling relatively thick samples) and in 3D reconstruction from serial images acquired along the z -axis.

2.2.4. Optical Sectioning Fluorescence Microscopy

An inherent limitation of traditional wide-field fluorescence imaging is the simultaneous excitation of fluorophores throughout the sample, both within and outside of the focal plane. As a result, out of focus light enters the detector and creates background “noise,” which convolutes the signal coming from fluorophores within the focal plane, thereby limiting resolution. Optical sectioning microscopy aims to eliminate this effect in order to improve resolution in the x - y plane and facilitate 3D reconstruction of samples via serial sectioning along the z -axis. Several distinct technologies have been developed to achieve optical sectioning, each offering distinct advantages and limitations, as discussed below (Table 2).

Table 2
Optical microscopy technologies

Technology^a	Advantage^b	Disadvantage/limitation^c	Primary use^d
Wide-field fluorescence (epifluorescence)	Sensitive Extremely flexible to broad applications Highly affordable	x - y and z resolution compromised by out-of-focus light	Live-cell imaging Diverse imaging of integrin and integrin-associated protein dynamics Integrin FRET studies
Laser-scanning confocal	Robust and high quality 3D imaging Generally quite flexible to broad applications	Long scan times Relatively high photo-toxicity Relatively high photo-bleaching	Optical sectioning Analytical co-localization studies of integrin & interacting proteins 3D-localization of integrins/ligands during cell-cell or cell-substrate interactions Integrin FRET studies
Spinning-disk confocal	Rapid scan times Relatively low photo-toxicity and photo-bleaching	Modest sensitivity Modest depth of field	Optical sectioning Live-cell 4D imaging in vitro Integrin FRET studies
Multiphoton	Excellent depth of field Limited photo-bleaching and photo-toxicity in thick samples	Long scan times Expensive	Optical sectioning Intravital 4D imaging Integrin function (adhesion & migration) in vivo Integrin FRET studies
TIRF	Outstanding axial resolution and contrast Relatively low photo-toxicity and photo-bleaching	Limited to the cell-substrate interface	Distribution dynamics of molecules at cell-substrate interface, especially adhesion structures Integrin FRET studies

Near-field scanning optical microscopy (NSOM)	Extremely high resolution (~20 nm x - y , ~5 nm z) Provide simultaneous optical & topological information	Low working distance and extremely shallow depth of field Limited to study of surfaces Long scan times Prone to artifacts Low sensitivity High skill required Highly specialized equipment	Imaging of nanoscale structures or single molecules Integrin diffusion dynamics Integrin organization into focal adhesions and raft domains
Far-field optical nanoscopy (FFON); 4pi, STED, SPEM, PALM, STORM	Extremely high resolution (~20 nm x - y , ~80 nm z) “Normal” working distances	Long scan times Requires photo-activatable or photo-switchable fluorophores Low sensitivity High skill required Highly specialized equipment Requires significant computational power/time	Imaging of nanoscale structures or single molecules Dynamics of focal adhesions

^aMajor types of optical microscopy imaging technologies listed. Extensive permutations by addition/combinations with additional hardware and computational approaches exist that are not shown

^bThe major strengths of each technology are listed

^cThe major weaknesses of each technology are listed

^dPrimary overall purpose and utility in the study of integrins

Laser-scanning fluorescence confocal microscopy (LSCM): Contrasting wide-field fluorescence, LSCM confocal microscope uses laser-mediated point illumination and a pinhole in an optically conjugate plane (i.e., “confocal”) in front of the detector to eliminate out-of-focus light (59). Since only a single point in the sample is excited at a time, 2D or 3D imaging requires raster scanning over the sample. No doubt, LSCM remains the most robust and versatile optical sectioning technology and has excelled in resolving static 3D structures and conduct analytical co-localization studies. However, LSCM also suffers from a range of limitations including relatively long scan times, high-energy excitation, and limited sensitivity (owing to the “wasted” photons rejected by the pinhole). In practice, the resulting photo-bleaching, photo-toxicity, and low temporal resolution make LSCM a relatively poor choice for time-lapse imaging of rapid events or of those requiring extended durations.

Spinning-disk fluorescence confocal microscopy (SDCM): Spinning (or Nipkow) disk confocal microscopy relies on the same basic principals as LSCM. However, SDCM replaces a rastering laser/pinhole system with a pair of disks arrayed with a series of pinholes spinning in unison (60, 61). The advantage to SDCM is that it offers much faster, indeed video rate, sectioning, and lower excitation energy than LSCM, thereby enabling time-lapse 3D imaging of samples (i.e., 4D imaging). However, the quality of imaging is inferior to LSCM and sensitivity is low compared to wide-field microscopy.

Multiphoton fluorescence microscopy (MPFM): Though often referred to as a “confocal” technology, MPFM, in fact, achieves optical sectioning in a manner fundamentally distinct from truly confocal microscopes (see above). The principal, instead, is to only excite fluorophores within the focal plane. This is achieved using mode-locked pulsed lasers that deliver low energy, long wavelength (specifically ~twice that of the fluorophore absorption maxima) photons that get driven into high density within ~1 μm of the focal plane (62). At such density, individual fluorophores have the opportunity to concomitantly absorb two or more photons providing sufficient energy for excitation (That is, a fluorophore that can be excited by a single photon of ~490 nm can alternatively be excited by concomitantly absorbing two photons of ~980 nm (each of which have twice the wavelength and half of the energy of a 490 nm photon)). Outside the focal plane little light absorption or excitation takes place because the density of photons is too low. This allows for much deeper penetration and greatly reduced photo-bleaching and photo-toxicity in thick samples. Moreover, since only fluorophores within the focal plane emit photons, MPFM can be used with direct detection systems (lacking pinholes), which significantly improves sensitivity. Taken together, the features of MPFM are ideally suited for intravital

imaging, where it has been exploited to characterize a variety of integrin-dependent processes such as leukocyte trafficking (63). It is important to note that for relatively thin samples, such as cultured cell monolayers, MPFM is largely similar to LSCM in terms of scan times, photo-toxicity, and photo-bleaching.

2.2.5. Total Internal Reflection Fluorescence Microscopy

Total internal reflection fluorescence (TIRF) microscopy is a unique technology that offers exceptionally high axial resolution (64). TIRF takes advantage of the fact that under conditions of total internal reflection (i.e., light striking an interface between materials of distinct refractive indices at sufficiently high incident angle) an evanescent energy wave is propagated perpendicular to the plane of the interface. The rapid exponential decay in energy intensity of this wave means that only fluorophores located very close to the cell–substrate interface can be excited, which effectively yields an axial resolution of ~100 nm (surpassing confocal or multiphoton optical sectioning by approximately five- to tenfold). That TIRF is inherently imaging only of the ventral cell–substrate interface makes it an ideal system for studying integrin substrate adhesion. Indeed, many studies (often coupled to other technologies) have exploited TIRF to characterize focal adhesion and podosome composition/dynamics, as well as integrin conformational states during adhesions (65–69).

2.2.6. Super-Resolution Optical Microscopy

Nanometer-scale resolution imaging has traditionally been the realm of electron, and more recently scanning probe (e.g., atomic force) microscopy (70). Resolution of optical microscopy has been characterized as being limited by diffraction (the process by which waves of light become distorted to create interference patterns as they pass through optical lenses). Thus, a single point source of light becomes blurred into a broader distribution of light intensities (that can be described by a point spread function; PSF), with maximal achievable resolution of ~200 nm in the x - y plain and ~600 nm along the z -axis (values that are inherently dictated by the wavelength of light). A range of technologies, broadly characterized as “near-field” and “far-field,” have overcome the diffraction limit and ushered in an emerging era of super/nano-resolution optical fluorescence microscopy (or “optical nanoscopy” (71)), which is already adding to our understanding of integrin-mediated functions.

Near-field scanning optical microscopy (NSOM/SNOM): NSOM was one of the first techniques to overcome the diffraction limit, and did so by exploiting the properties of evanescent waves. In NSOM, a nanometer-scale detector is placed at a very short distance (also on the scale of nanometers) to the specimen surface. With this technique, the resolution of the image is limited by the size of the detector aperture rather than the excitation wavelength,

yielding lateral resolution of 20 nm and vertical resolution of 2–5 nm (72, 73). Furthermore, because of the extremely small near-field excitation volume (and therefore reduced background fluorescence from the cytoplasm), NSOM sensitivity extends to the level of single molecule detection. The downside, however, to this feature is that this technique is limited to imaging of the sample surface. NSOM is also generally quite requires highly specialized equipment/expertise and has, therefore, been applied only to a limited degree. Nonetheless, NSOM has provided insights to integrin behavior (73). Specifically, NSOM has been exploited to analyze the spatio-functional relationship between the integrin LFA-1 and lipid raft components (GPI-APs) on immune cells. Such studies revealed previously unappreciated nanoscale building blocks and hierarchical aggregation pathways driving activation/ligand-dependent integrin clustering (72, 73).

Far-field optical nanoscopy (FFON): Contrasting NSOM, FFON (as the name implies) allows nanoscale resolution at working distances similar to those for most other types of optical microscopy. FFON is not a single technique but rather a term that captures a collection of diverse approaches (such as, 4pi, STED, SPEM, PALM, and STORM) being developed for nanoscale optical imaging (71, 74). Among these, PALM (photo-activated localization microscopy (66, 67, 75)) and STORM (Sub-diffraction-limit imaging by stochastic optical reconstruction microscopy (76)) seem to show the most promise. These both take advantage of recent advances such as the development of photo-switchable fluorophores, high-sensitivity microscopes, and single particle localization algorithms to achieve resolution of several nanometers. At the moment, these approaches remain rather sophisticated requiring highly specialized equipment and expertise and additionally require substantial off-line computational time/power (Table 2) (71, 74). There are also a number of limitations in the experimental setup, such as need for photo-switchable fluorophores, that are nontrivial.

Despite the limitations, FFOM represents an exciting frontier in bio-imaging that has already shown utility in the study of integrins and adhesion biology. Among the first applications of FFOM was the use of PALM to visualize vinculin in focal adhesions and actin within a lamellipodium of fixed cells with 2–25 nm resolution (75). Shortly thereafter, PALM was used to investigate nanoscale dynamics within individual adhesion complexes (ACs) in living cells under physiological conditions (66, 67). In this study, AC dynamics were visualized (with 25 s temporal resolution and 60 nm spatial resolution) allowing measurement of the fractional gain and loss of individual paxillin and vinculin molecules as each AC evolved (66, 67).

2.3. Advanced Fluorescence Imaging Modalities

As discussed above diversity in imaging comes from the intersection of technologies and the means by which these are applied (i.e., “modalities”). Whereas the former emphasizes the role of hardware and fundamental capabilities of equipment (Table 2), the later emphasizes image acquisition/processing protocols and experimental design features such as choice of fluorescent probe and how these are introduced into the system and subsequently manipulated. The most rudimentary imaging modalities involve determining subcellular distribution of molecules and/or organelles of interest with respect to each other, often during dynamic processes such as adhesion and migration. A wide range of advanced imaging modalities have been developed that allow for discrete aspects of molecular behavior to be probed. Below, we focus on those most extensively exploited (or show important potential) for understanding integrins.

2.3.1. Fluorescence (or “Forster”) Resonance Energy Transfer

FRET microscopy encompasses multiple techniques that allow for nanometer-scale conformational changes or intermolecular interactions to be probed with high spatial and (often) temporal resolution in intact cells (77, 78) (Fig. 2d). As described above (Subheading 2.2.1), fluorophores “borrow” photons of particular wavelengths for a short period of time before releasing photons of longer wavelengths (i.e., of lower energy). FRET takes advantage of the process described by Theodor Forster in which appropriately matched “donor” and “acceptor” fluorophores can directly pass energy on through “resonance” without intermediate release of photons when they are in close physical juxtaposition (i.e., ~2–10 nm apart) (Fig. 2d) (77, 78). As a result, the emitted donor wavelength is “quenched” by the acceptor resulting in “sensitized” fluorescence emission at the acceptor emission wavelength. In practice FRET can be measured by monitoring the ratio of donor and acceptor emission (ratiometric FRET), the quenching of the donor emission or the fluorescence lifetime of the donor.

Fluorescence lifetimes can be monitored by FLIM (fluorescence lifetime imaging microscopy), which makes use of pulsed lasers (such as those used in MPFM, above) to induce temporally discrete excitation events and then measures fluorescence lifetimes through so-called time domain or frequency domain methods (77, 78). FLIM-FRET takes advantage of the fact that fluorescence lifetime decreases proportionally to the efficiency of FRET. FLIM-FRET is generally regarded as the gold standard for FRET analysis (due to its relative freedom from artifacts, such as those associated with spectral cross-talk and donor/acceptor concentration), as well as its high temporal and spatial resolution. However, this method also requires the most sophisticated (and expensive) equipment, along with the highest degree of expertise.

Next to FLIM-FRET, the “donor de-quenching” (or “acceptor photo-bleach”) method provides the best accuracy/freedom from artifacts and is compatible with most imaging technologies and experimental designs (i.e., with respect to types of biomolecules and probes that can be used as donor and acceptor) (77, 78). This method basically measures donor fluorescence before and after photo-bleaching of the acceptor (which effectively destroys the acceptor, thereby removing its quenching effect). The relative increase in the fluorescence in the “de-quenched” donor is proportional to FRET efficiency. The obvious downside to this methodology is that it is an endpoint measurement and, thus, is incompatible with dynamic monitoring within the same sample.

When used with appropriate spectral cross-talk correction, ratiometric FRET offers an easy option for dynamic measurements. However, this method is only appropriate in settings of specific “biosensors” engineered to contain donor and acceptor (typically Cyan FP (CFP) and Yellow FP (YFP)) in the same molecule. This ensures that the molar ratio of donor and acceptor in cells and any local volume is constant.

Finally, a variation of FRET termed BRET (Bioluminescence Resonance Energy Transfer) has been developed (79). This technique uses a bioluminescent luciferase to produce initial photon emission, serving effectively as a donor, compatible with green and yellow acceptors. The advantage of BRET is that no excitation light is required, thereby avoiding photo-bleaching and photo-toxicity. However, BRET is also constrained by kinetics of the luciferase enzymatic activity.

FRET studies of integrin conformation: cytoplasmic domain separation: As discussed in Subheading 1.2, early EM and crystal structures suggested the hypothesis that integrin regulation involved large-scale (on the order of ~3–10 nm) conformational rearrangement that would specifically involve separation of the α and β subunits legs and extension of the head domain away from the plasma membrane (Fig. 1a). One of the first studies to test the validity of this hypothesis in intact cells used a FRET-based approach in which the C-termini of the α and β subunits were differentially fused to CFP and YFP to serve as FRET donor and acceptor, respectively (Fig. 3a). Using a photo-bleach FRET approach, it was demonstrated in live cells that, in fact, in the resting state the cytoplasmic domains of LFA-1 were close to each other and that they underwent significant spatial separation upon either activation or ligand binding (13). A similar FRET approach was subsequently employed in conjunction with mutagenesis in to demonstrate that the LFA-1 transmembrane domains play an important role in this conformational regulation (80). Additional studies using the cytoplasmic FRET approach with the integrin Mac1 demonstrate that constitutive heterodimerization of α M

and $\beta 2$ subunits is detectable in plasma membrane, peri-nuclear area, and Golgi in living cells (81) and that interaction of Mac1 in the extracellular domain with uPAR (glycosylphosphatidylinositol-linked urokinase-type plasminogen activator receptor) promotes conversion into the open conformation (82). Finally, the cytoplasmic FRET approach was applied to demonstrate specific zones in the leading edge where activation of the integrin VLA-4 is concentrated during lateral migration (65).

FRET studies of integrin conformation: head extension: As discussed above, in addition to leg separation, integrins were hypothesized to have a strongly bent extracellular domain on the cell surface in the resting state that undergoes large-scale extension during activation (Fig. 1a). To test this aspect of the conformational model, again FRET was applied (52). Here a fluorescein-conjugated peptide ligand that specifically binds to the VLA-4 (in the ligand-binding head domain) served as the FRET donor and a lipophilic dye, octadecyl rhodamine B, was incorporated into the plasma membrane to serve as a FRET acceptor (Fig. 3b) (52). These studies confirmed in intact cells that the head domain in resting cells lies close to the plasma membrane but is rapidly extended away from it upon activation (52) (83). A similar assay was developed for LFA-1 using a fluorescent derivative of the small molecule head domain-binding agonist BIRT-377 (53). Recent studies have applied Alexa488- and Cy3-conjugated fAb fragments (specific for the β subunit “I-like” domain and α subunit “calf” domain) to create more refined characterization of the conformational changes within the extracellular domain during activation of the platelet integrin α IIB β 3 (84).

FRET studies of integrin microclustering: To assess integrin microclustering variations on the cytoplasmic domain assays discussed above have been developed (17, 18, 79, 85). In such systems, rather than attaching donor and acceptor differentially to a and b subunits, donor and acceptor are placed either both on the α or both on the β subunit (Fig. 3c). Thus, individual integrin heterodimers will possess a single donor or acceptor and FRET will only occur when two of these come into close proximity. Such systems have been instrumental in determining mechanisms that microclustering. For example, the role of ligand in driving microclustering was demonstrated by the finding that PMA, cytochalasin-D and latrunculin, at concentrations that activate adhesion and diffusivity (20) do not promote BRET-detectable microclustering of α IIB β 3 (79) or FRET-detectable microclustering of LFA-1 (85), whereas addition of soluble multivalent ligands readily induces microclustering of these integrins. Additional studies suggest that the $\beta 2$ transmembrane domains (and particularly residue Thr-686) play important roles in driving homomeric associations for integrins Mac1 (17) and LFA-1 (18).

In addition, a unique FRET-based assay to monitor integrin microclustering was developed in which extracellular YFP and dsRed (FRET donor and acceptor, respectively) each fused to β integrin transmembrane/cytoplasmic domains were co-expressed with full-length integrin heterodimers (86). In this system, FRET increased during adhesion to ligand. Since the FRET reporters lack ligand-binding capability, these results support the idea that ligand-driven microclustering may be propagated, at least in part, through indirect mechanisms that are downstream of the actual ligand-binding event (e.g., conformational changes in heterodimers or outside-in signaling) (86).

FRET studies of integrin heterotypic protein binding: It is clear that interactions between integrin cytoplasmic domains and both the cytoskeleton and various signaling molecules are altered dynamically as part of both inside-out and outside-in signaling. Integrins also mediated lateral associations with other membrane proteins that may modulate function. In order to study the temporal and spatial dynamics of these interactions, FRET-based assays have been designed in which FP FRET donors and acceptors are differentially incorporated into the cytoplasmic domain of one of the integrin subunits and a target molecule (Fig. 3d). In this way, through use of a FLIM-FRET assay, it was shown that formation of an integrin- $\alpha 4/14-3-3z$ /paxillin protein ternary complex mediates localized Cdc42 activity and accelerates cell migration (87). Similarly, FRET studies have been developed to measure $\beta 1$ -integrin lateral association with ErbB2 kinase (88) and cytoplasmic association with PKC α (89). Moreover, FLIM-FRET has been developed to quantify integrin receptor agonism using $\beta 1$ integrin-GFP and effector-mRFP interactions as a readout (90). Thus, association of talin with $\beta 1$ integrin and paxillin with $\alpha 4$ integrin was demonstrated to be dependent on both the ligand and receptor activation state, and sensitive to inhibition with small molecule RGD and LDV mimetics, respectively (90).

FRET studies of integrin signaling: FRET assays have also proven useful in understanding protein complexes and signaling events downstream of integrins using diverse experimental designs and biosensors (77). For example, biosensors that report activity of Rho family GTPases involved in integrin signaling (e.g., Rho, Rac, Cdc42, and Rap) have been used to understand localized signaling during integrin-dependent adhesion and migration (77). Additionally, FRET has been used to characterize signaling through integrin cytoplasmic domain-associated protein-1 (ICAP-1). ICAP-1 binds to both $\beta 1$ integrin and the ROCK kinase (an effector of the RhoA GTPase) through separate domains (91). FRET between CFP-ICAP-1 and YFP-ROCK demonstrated that ICAP-1 could serve as a scaffold to drive indirect ROCK- $\beta 1$ integrin interactions (within specific leading and trailing edge regions) that are important for properly orchestrated

cell migration (91). Finally, the importance of temporal and spatial negative regulation of α IIb β 3 signaling for proper cell spreading was elucidated in part through FRET assays that report interactions between Src-YFP and CFP-Csk (positive and negative regulators, respectively, of signaling) (92).

2.3.2. Fluorescence Recovery After Photo-Bleaching

FRAP, and the related method FLIP (Fluorescence Loss in Photo-bleaching), are modes of measuring *en mass* diffusiveness of proteins within cells or within membranes of cells (Fig. 4). In FRAP, the movement of fluorescent species into a region acutely subjected to photo-bleaching (Fig. 4a) is monitored. In FLIP, a region is continuously subjected to photo-bleaching, while the depletion of fluorescence in a region outside the bleaching zone is monitored. A recent variation on these approaches involves the use of photo-activatable or photo-switchable FPs, which can be locally activated/switched within a limited zone in order to assess subsequent movement out of that zone. The two most important parameters that can be extracted from these methods are diffusion coefficients (rate at which fluorescent species move into or out of the monitored zone) and the mobile fraction (the percentage of fluorescent species that undergoes detectable movement) (Fig. 4b).

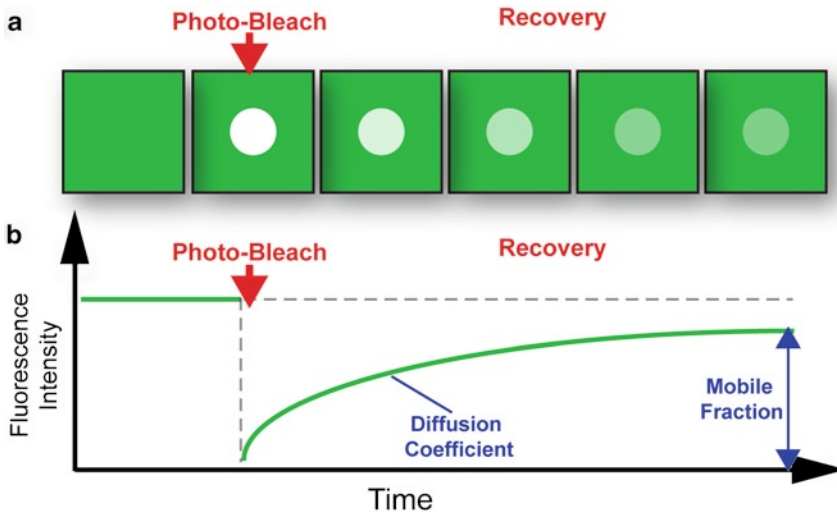


Fig. 4. Fluorescence Recovery After Photo-Bleaching (FRAP). FRAP is one of the most broadly used techniques to monitor molecular mobility of biomolecules, including integrin, in intact live-cell settings. (a) Basic FRAP approach. Green panels represent a cellular region containing fluorescent molecules (e.g., plasma membrane-bound integrin-GFP). The *first panel* on the *left* depicts baseline intensity. The *next panel* depicts the discrete photo-bleaching of a sub-region (most typically by an intense burst of laser excitation light). *Subsequent panels* show time-dependent recovery of fluorescence intensity within the bleached region. (b) FRAP analysis. The plot depicts a typical intensity profile during a FRAP experiment. The recovery curve provides a basis for calculating overall diffusion coefficients. The saturation point of the recovery curve provides an estimate for the overall fraction of the fluorescent molecules that exhibit detectable diffusion. When applied to integrins, inverse population, the immobile fraction, often represents to the proportion tethered to the cytoskeleton.

For integrins, diffusion rates/immobilization are critical determinant of their adhesive functions (5, 7, 19–23, 32, 35–38, 68). FRAP-based approaches have been widely employed to integrins in order to demonstrate the roles of inside-out signals, cytoskeletal tethering and integrin conformation in altering diffusivity and how this is related to adhesive dynamics (38, 85, 93).

2.3.3. Fluorescence Speckle Imaging

Among the methods to study molecular dynamics in cells FRAP-based studies (which measures whole population of molecules *en mass*) and single molecule fluorescence/SPT could be viewed as representing extremes. A novel methodology termed fluorescence speckle microscopy (FSM) might be viewed as representing an intermediate approach that offers unique advantages that are particularly useful in cytoskeletal and adhesion biology (60, 94). At high concentration, fluorescent tags illuminate cytoskeletal polymers uniformly. However, at low concentration (when percentage of tagged to endogenous molecules is $\leq 1\%$), random incorporation of tags produces a discontinuous pattern, which can then be used to determine whether the polymer is translocating or stationary. In practice, FSM conditions are achieved either by injecting very low concentrations of fluorescently tagged proteins or, for GFP-coupled proteins, adjusting conditions so that only small amounts of the labeled protein are expressed. Detection of speckles requires a sensitive microscopy system (which under optimal conditions can detect single fluorophores) and sophisticated correlation algorithms.

Some of the first studies to use FSM focused on the coupling of focal-adhesion proteins to actin filaments (95). These studies revealed classes of focal-adhesion structural and regulatory molecules that correlated with motions actin filaments to varying degrees (95). From these studies it was inferred that interactions between vinculin, talin, and actin filaments constitute a sort of “molecular clutch” between the cytoskeleton and integrins, which is regulated during cell migration (95).

2.3.4. Chromophore-Assisted Light Inactivation

CALI is a relatively novel fluorescence method that takes advantage of the oxidative processes associated with fluorescence, i.e., phototoxicity (96). Irradiation of fluorescent molecules, such as GFP, effectively causes photo-synthesis of ROS, which can damage nearby proteins, and especially the target molecule to which the FP may be fused. Thus, by fusion a target molecule of interest with an FP and then irradiating it with intense laser excitation one can selectively destroy the target in intact cells. Though initial studies have been conducted with GFP (see below), several newly identified/engineered FPs, such as Killer Red, show strongly enhanced (up to 1,000-fold over GFP) photo-synthesis of ROS suggesting even greater potential for future CALI applications (96).

Some of the first CALI studies were centered on understanding of focal adhesions (97). Here Swiss 3T3 cells expressing EGFP- α -actinin (but not those expressing EGFP-FAK) exhibited detachment of stress fibers from focal adhesions upon focused laser irradiation. CALI experiments also demonstrated a reduction of EGFP- α -actinin binding to the cytoplasmic domain of the β 1 integrin subunit, but not to actin. Thus, CALI was able to provide unique demonstration that α -actinin is essential for the binding of microfilaments to integrins in focal adhesions (97).

2.3.5. Toward Imaging Force and Mechano-Transduction

An inherent aspect of integrin function is the ability to resist and transduce forces, as well as its ability to serve as “mechano-sensors” that transduce mechanical force information into biochemical signals (“mechano-transduction”). These features are increasingly appreciated as central aspects of integrin regulation (98–101). Methods to assess responses to integrin-mediated mechano-transduction have largely been through whole sample biochemical (e.g., kinase and Rho-family GTPase activation assays) or gene expression analysis (98–101). However, since the very essence of mechano-transduction is the sensing of spatially and temporally discrete force application events, such whole sample methods are clearly missing critical information. Imaging modalities to better understand the spatial/temporal orchestration of integrin mechano-transduction responses are only beginning to be developed and involves varied approaches (94, 98–101).

One intuitive approach to imaging integrin mechano-transduction is to simply monitor morphologic, protein distribution and signaling responses to application of a mechanical stimulus. In addition to various integrin/intergrin-associated localization probes (discussed above), a wide range of FRET-based probes have been generated (that involve integrins (see above), vinculin, Myosin II, N-WASP, many Rho-family GTPases and kinases) that have utility in the study of mechano-transduction (102). For example, a FRET biosensor for Src kinase activity was used in conjunction with locally applied pulling forces on integrins, via laser-tweezer traction or “magnetic twisting” of fibronectin-coated beads adhering to cell surfaces (103–105). These studies revealed the transmission of mechanically induced Src activation in a dynamic and directed process that relies on the cytoskeleton (103–105). In another study, cellular reorganization of focal adhesions and cytoskeleton was monitored in parallel with FRET-based RhoA, Rac1, and Cdc42 activity biosensors. These studies showed that application of cyclic stretching forces drives dramatic reorganization of focal adhesions and the actin cytoskeleton that correlated with strong increase in RhoA, but not Rac1 or Cdc42 (106).

Other approaches seek to visualize the genesis of traction forces. For example, Spatio-temporal image correlation spectroscopy

(STICS), uses correlation algorithms assesses directed movement of fluorescently tagged proteins and generate high-resolution velocity maps of adhesion components during force generation. Maps for actin, α -actinin, $\alpha 5$ -integrin, talin, paxillin, vinculin, and focal adhesion kinase revealed significant differences in the efficiency of the linkage between integrin and actin among different cell types and on the same cell type grown on different substrate densities during formation of adhesions and traction forces (107). Additionally, studies have developed correlative motion-sensing approaches to directly visualize force generation. High resolution traction force microscopy is one such method that uses fluorescent nano-beads introduced into deformable polyacrylamide gels (used as a cell adhesion substrate) which serve as markers for substrate deformation, the motion of which can be computationally transformed into force vector maps (108). Studies using combined traction force and fluorescent speckle microscopy, demonstrated that F-actin speed is a fundamental and biphasic regulator of traction force at focal adhesions during cell migration. That is, F-actin speed was inversely related to traction stress near the cell edge, where focal adhesions are formed and F-actin motion is rapid. In contrast, larger focal adhesions (where the F-actin speed is low) were marked by a direct relationship between F-actin speed and traction stress (109).

3. Summary and Perspective

Integrins are extremely dynamic adhesion/signaling receptors with diverse modes of regulation. Because integrin behavior is inherently coupled to temporally and spatially discrete organization patterns, imaging approaches capable of providing dynamic subcellular spatial resolution are absolutely essential to elucidating integrin function. Traditional and emerging imaging technologies/modalities have been employed diversely in an effort to address the many distinct aspects of integrin function. In this way, major components of integrin conformational regulation, micro-clustering, protein-protein interactions and cellular distribution dynamics have been elucidated in intact cell systems. Moving forward, continued development of multidimensional approaches (e.g., that coordinately report cell migration behavior, integrin localization, integrin conformation, and signaling processes) represents a feasible (and perhaps the only) way to understand how integrin functions are orchestrated in cells. In addition, continued application of existing, and development of novel, modalities to image mechano-transduction is now recognized as a particularly important goal in integrin adhesion biology. The rapid advances in imaging technologies and computational power/

approaches, along with the growing collection of fluorescent probes and biosensors, suggest, at least over the short term, that available imaging modalities for studying integrins will only be limited by the creativity of the investigator.

Acknowledgments

This work was supported by the Arthritis Foundation, American Heart Association, and Roche Organ Transplant Research Foundation.

References

1. Luo, B.-H., Carman, C. V., and Springer, T. A. (2007) Structural basis of integrin regulation and signaling, *Annu. Rev. Immunol.* **25**, 619–647.
2. Nermut, M. V., Green, N. M., Eason, P., Yamada, S. S., and Yamada, K. M. (1988) Electron microscopy and structural model of human fibronectin receptor, *EMBO J.* **7**, 4093–4099.
3. Xiong, J.-P., Stehle, T., Diefenbach, B., Zhang, R., Dunker, R., Scott, D. L., Joachimiak, A., Goodman, S. L., and Arnaout, M. A. (2001) Crystal structure of the extracellular segment of integrin $\alpha V\beta 3$, *Science* **294**, 339–345.
4. Xiong, J. P., Stehle, T., Zhang, R., Joachimiak, A., Frech, M., Goodman, S. L., and Arnaout, M. A. (2002) Crystal structure of the extracellular segment of integrin $\alpha V\beta 3$ in complex with an Arg-Gly-Asp ligand, *Science* **296**, 151–155.
5. Carman, C. V., and Springer, T. A. (2003) Integrin avidity regulation: Are changes in affinity and conformation underemphasized?, *Curr. Opin. Cell Biol.* **15**, 547–556.
6. Miranti, C. K., and Brugge, J. S. (2002) Sensing the environment: a historical perspective on integrin signal transduction, *Nat. Cell Biol.* **4**, E83–90.
7. Constantin, G., Majeed, M., Giagulli, C., Piccib, L., Kim, J. Y., Butcher, E. C., and Laudanna, C. (2000) Chemokines trigger immediate $\beta 2$ integrin affinity and mobility changes: differential regulation and roles in lymphocyte arrest under flow, *Immunity* **13**, 759–769.
8. Chan, J. R., Hyduk, S. J., and Cybulsky, M. I. (2001) Chemoattractants induce rapid and transient upregulation of monocyte $\alpha 4$ integrin affinity for vascular adhesion molecule 1 which mediates arrest: an early step in the process of emmigration, *J. Exp. Med.* **193**, 1149–1158.
9. Chan, J. R., Hyduk, S. J., and Cybulsky, M. I. (2003) Detecting rapid and transient upregulation of leukocyte integrin affinity induced by chemokines and chemoattractants, *J. Immunol. Meth.* **273**, 43–52.
10. Shimaoka, M., Kim, M., Cohen, E. H., Yang, W., Astrof, N., Peer, D., Salas, A., Ferrand, A., and Springer, T. A. (2006) AL-57, a ligand-mimetic antibody to integrin LFA-1, reveals chemokine-induced affinity up-regulation in lymphocytes, *Proc. Natl. Acad. Sci. USA* **103**, 13991–13996.
11. Takagi, J., Petre, B. M., Walz, T., and Springer, T. A. (2002) Global conformational rearrangements in integrin extracellular domains in outside-in and inside-out signaling, *Cell* **110**, 599–611.
12. Takagi, J., Strokovich, K., Springer, T. A., and Walz, T. (2003) Structure of integrin $\alpha 5\beta 1$ in complex with fibronectin, *EMBO J.* **22**, 4607–4615.
13. Kim, M., Carman, C. V., and Springer, T. A. (2003) Bidirectional transmembrane signaling by cytoplasmic domain separation in integrins, *Science* **301**, 1720–1725.
14. Xiao, T., Takagi, J., Wang, J.-h., Collier, B. S., and Springer, T. A. (2004) Structural basis for allostery in integrins and binding of ligand-mimetic therapeutics to the platelet receptor for fibrinogen, *Nature* **432**, 59–67.
15. Li, R., Babu, C. R., Lear, J. D., Wand, A. J., Bennett, J. S., and Degrado, W. F. (2001) Oligomerization of the integrin $\alpha IIb\beta 3$: Roles of the transmembrane and cytoplasmic domains, *Proc. Natl. Acad. Sci. USA* **98**, 12462–12467.

16. Li, R., Mitra, N., Gratkowski, H., Vilaire, G., Litvinov, S. V., Nagasami, C., Weisel, J. W., Lear, J. D., DeGrado, W. F., and Bennett, J. S. (2003) Activation of integrin α IIb β 3 by modulation of transmembrane helix associations, *Science* **300**, 795–798.
17. Fu, G., Wang, C., Wang, G. Y., Chen, Y. Z., He, C., and Xu, Z. Z. (2006) Detection of constitutive homomeric associations of the integrins Mac-1 subunits by fluorescence resonance energy transfer in living cells, *Biochem. Biophys. Res. Commun.* **351**, 847–852.
18. Vararattanavech, A., Lin, X., Torres, J., and Tan, S. M. (2009) Disruption of the integrin α L β 2 transmembrane domain interface by β 2 Thr-686 mutation activates α L β 2 and promotes micro-clustering of the α L subunits, *J. Biol. Chem.* **284**, 3239–3249.
19. Jin, T., and Li, J. (2002) Dynamitin controls β 2 integrin avidity by modulating cytoskeletal constraint on integrin molecules, *J. Biol. Chem.* **277**, 32963–32969.
20. Kucik, D. F., Dustin, M. L., Miller, J. M., and Brown, E. J. (1996) Adhesion-activating phorbol ester increases the mobility of leukocyte integrin LFA-1 in cultured lymphocytes, *J. Clin. Invest.* **97**, 2139–2144.
21. Peters, I. M., van Kooyk, Y., van Vliet, S. J., de Grooth, B. G., Figdor, C. G., and Greve, J. (1999) 3D single-particle tracking and optical trap measurements on adhesion proteins, *Cytometry* **36**, 189–194.
22. Smith, A., Carrasco, Y. R., Stanley, P., Kieffer, N., Batista, F. D., and Hogg, N. (2005) A talin-dependent LFA-1 focal zone is formed by rapidly migrating T lymphocytes, *J. Cell Biol.* **170**, 141–151.
23. Felsenfeld, D. P., Choquet, D., and Sheetz, M. P. (1996) Ligand binding regulates the directed movement of β 1 integrins on fibroblasts, *Nature* **383**, 438–440.
24. Leitinger, B., and Hogg, N. (2001) The involvement of lipid rafts in the regulation of integrins function, *J. Cell Sci.* **115**, 963–972.
25. Hogg, N., Henderson, R., Leitinger, B., McDowall, A., Porter, J., and Stanley, P. (2002) Mechanisms contributing to the activity of integrins on leukocytes, *Immunol. Rev.* **186**, 164–171.
26. Shamri, R., Grabovinsky, V., Feigelson, S. W., Dwir, O., van Kooyk, Y., and Alon, R. (2002) Chemokine stimulation of lymphocyte α_4 integrin avidity but not leukocyte functional-associated antigen-1 avidity to endothelial ligands under shear flow requires cholesterol membrane rafts, *J. Biol. Chem.* **277**, 40027–40035.
27. Krauss, K., and Altevogt, P. (1999) Integrin leukocyte function-associated antigen-1-mediated cell binding can be activated by clustering of membrane rafts, *J. Biol. Chem.* **274**, 36921–36927.
28. Hemler, M. E. (2003) Tetraspanin proteins mediate cellular penetration, invasion, and fusion events and define a novel type of membrane microdomain, *Annu. Rev. Cell Devel. Bio.* **19**, 397–422.
29. Petty, H. R., Worth, R. G., and Todd, R. F. r. (2002) Interactions of integrins with their partner proteins in leukocyte membranes, *Immunol. Res.* **25**, 75–95.
30. Shattil, S. J., P. J. Newman. (2004) Integrins: dynamic scaffolds for adhesion and signaling in platelets, *Blood* **104**, 1606–1615.
31. Grashoff, C., Thievensen, I., Lorenz, K., Ussar, S., and Fassler, R. (2004) Integrin-linked kinase: integrin's mysterious partner, *Curr. Opin. Cell Biol.* **16**, 565–571.
32. Ridley, A. J., Schwartz, M. A., Burridge, K., Firtel, R. A., Ginsberg, M. H., Borisy, G., Parsons, J. T., and Horwitz, A. R. (2003) Cell migration: integrating signals from front to back, *Science* **302**, 1704–1709.
33. Guo, W., and Giancotti, F. G. (2004) Integrin signalling during tumour progression, *Nat. Rev. Mol. Cell Biol.* **5**, 816–826.
34. Zhu, J., Carman, C. V., Kim, M., Shimaoka, M., Springer, T. A., and Luo, B. H. (2007) Requirement of alpha and beta subunit transmembrane helix separation for integrin outside-in signaling, *Blood* **110**, 2475–2483.
35. Plancon, S., Morel-Kopp, M. C., Schaffner-Reckinger, E., Chen, P., and Kieffer, N. (2001) Green fluorescent protein (GFP) tagged to the cytoplasmic tail of α IIb or β 3 allows the expression of a fully functional integrin α IIb β 3: effect of β 3GFP on α IIb β 3 ligand binding, *Biochem. J.* **357**, 529–536.
36. Laukaitis, C. M., Webb, D. J., Donais, K., and Horwitz, A. F. (2001) Differential dynamics of α 5 integrin, paxillin, and α -actinin during formation and disassembly of adhesions in migrating cells, *J. Cell Biol.* **153**, 1427–1440.
37. Dustin, M. L. (2009) Supported bilayers at the vanguard of immune cell activation studies, *J. Struct. Biol.* **168**, 152–160.
38. Cairo, C. W., Mirchev, R., and Golan, D. E. (2006) Cytoskeletal regulation couples LFA-1 conformational changes to receptor lateral mobility and clustering, *Immunity* **25**, 297–308.
39. Lawson, M. A., and Maxfield, F. R. (1995) Ca^{2+} - and calcineurin-dependent recycling of

- an integrin to the front of migrating neutrophils, *Nature* **377**, 75–79.
40. Tohyama, Y., Katagiri, K., Pardi, R., Lu, C., Springer, T. A., and Kinashi, T. (2003) The critical cytoplasmic regions of the α L/ β 2 integrin in Rap1-induced adhesion and migration, *Mol. Biol. Cell* **14**, 2570–2582.
 41. Katagiri, K., Maeda, A., Shimonaka, M., and Kinashi, T. (2003) RAPL, a novel Rap1-binding molecule, mediates Rap1-induced adhesion through spatial regulation of LFA-1, *Nat. Immunol.* **4**, 741–748.
 42. Shimonaka, M., Katagiri, K., Kakayama, T., Fujita, N., Tsuruo, T., Yoshie, O., and Kinashi, T. (2003) Rap1 translates chemokine signals to integrin activation, cell polarization, and motility across vascular endothelium under flow, *J. Cell Biol.* **161**, 417–427.
 43. Centonze Frohlich, V. (2008) Phase contrast and differential interference contrast (DIC) microscopy, *J. Vis. Exp.* **6**, 844.
 44. Verschueren, H. (1985) Interference reflection microscopy in cell biology: Methodology and applications, *J. Cell. Sci.* **75**, 279–301.
 45. Bailly, M., Condeelis, J. S., and Segall, J. E. (1998) Chemoattractant-induced lamellipod extension, *Microsc. Res. Tech.* **43**, 433–443.
 46. Neumeister, P., Pixley, F. J., Xiong, Y., Xie, H., Wu, K., Ashton, A., Cammer, M., Chan, A., Symons, M., Stanley, E. R., and Pestell, R. G. (2003) Cyclin D1 governs adhesion and motility of macrophages, *Mol. Biol. Cell* **14**, 2005–2015.
 47. Linder, S. (2009) Invadosomes at a glance, *J. Cell Sci.* **122**, 3009–3013.
 48. Ritchie, K., and Kusumi, A. (2003) Single-particle tracking image microscopy, *Meth. Enzymol.* **360**, 618–634.
 49. Giepmans, B. N., Adams, S. R., Ellisman, M. H., and Tsien, R. Y. (2006) The fluorescent toolbox for assessing protein location and function, *Science* **312**, 217–224.
 50. Wang, Y., Shyy, J. Y., and Chien, S. (2008) Fluorescence proteins, live-cell imaging, and mechanobiology: seeing is believing, *Annu Rev. Biomed. Eng.* **10**, 1–38.
 51. Bonasio, R., Carman, C. V., Kim, E., Sage, P. T., Love, K. R., Mempel, T. R., Springer, T. A., and von Andrian, U. H. (2007) Specific and covalent labeling of a membrane protein with organic fluorochromes and quantum dots, *Proc. Natl. Acad. Sci. USA.* **104**, 14753–14758.
 52. Chigaev, A., Buranda, T., Dwyer, D. C., Prossnitz, E. R., and Sklar, L. A. (2003) FRET detection of cellular α 4-integrin conformational activation, *Biophys J.* **85**, 3951–3962.
 53. Larson, R. S., Davis, T., Bologna, C., Semenuk, G., Vijayan, S., Li, Y., Oprea, T., Chigaev, A., Buranda, T., Wagner, C. R., and Sklar, L. A. (2005) Dissociation of I domain and global conformational changes in LFA-1: refinement of small molecule-I domain structure-activity relationships, *Biochemistry* **44**, 4322–4331.
 54. Barreiro, O., Yanez-Mo, M., Serrador, J. M., Montoya, M. C., Vicente-Manzanares, M., Tejedor, R., Furthmayr, H., and Sanchez-Madrid, F. (2002) Dynamic interaction of VCAM-1 and ICAM-1 with moesin and ezrin in a novel endothelial docking structure for adherent leukocytes, *J. Cell Biol.* **157**, 1233–1245.
 55. Carman, C. V., Jun, C. D., Salas, A., and Springer, T. A. (2003) Endothelial cells proactively form microvilli-like membrane projections upon intercellular adhesion molecule 1 engagement of leukocyte LFA-1, *J. Immunol.* **171**, 6135–6144.
 56. Carman, C. V., and Springer, T. A. (2004) A transmigratory cup in leukocyte diapedesis both through individual vascular endothelial cells and between them, *J. Cell Biol.* **167**, 377–388.
 57. Carman, C. V., Sage, P. T., Sciuto, T. E., de la Fuente, M. A., Geha, R. S., Ochs, H. D., Dvorak, H. F., Dvorak, A. M., and Springer, T. A. (2007) Transcellular diapedesis is initiated by invasive podosomes, *Immunity* **26**, 784–797.
 58. Yang, L., Froio, R. M., Sciuto, T. E., Dvorak, A. M., Alon, R., and Luscsinkas, F. W. (2005) ICAM-1 regulates neutrophil adhesion and transcellular migration of TNF- α -activated vascular endothelium under flow, *Blood* **106**, 584–592.
 59. Paddock, S. W. (1999) An introduction to confocal imaging, *Meth. Mol. Biol.* **122**, 1–34.
 60. Maddox, P. S., Moree, B., Canman, J. C., and Salmon, E. D. (2003) Spinning disk confocal microscope system for rapid high-resolution, multimode, fluorescence speckle microscopy and green fluorescent protein imaging in living cells, *Meth. Enzymol.* **360**, 597–617.
 61. Graf, R., Rietdorf, J., and Zimmermann, T. (2005) Live cell spinning disk microscopy, *Adv. Biochem. Eng. Biotechnol.* **95**, 57–75.
 62. Rubart, M. (2004) Two-photon microscopy of cells and tissue, *Circulation Res.* **95**, 1154–1166.
 63. Zarbock, A., and Ley, K. (2009) New insights into leukocyte recruitment by intravital microscopy, *Curr. Top. Microbiol. Immunol.* **334**, 129–152.

64. Fish, K. N. (2009) Total internal reflection fluorescence (TIRF) microscopy, *Current Protoc. Cytometry* J. Paul Robinson, Ed. Chapter 12, Unit 12.18.
65. Hyun, Y. M., Chung, H. L., McGrath, J. L., Waugh, R. E., and Kim, M. (2009) Activated integrin VLA-4 localizes to the lamellipodia and mediates T cell migration on VCAM-1, *J. Immunol.* **183**, 359–369.
66. Shroff, H., Galbraith, C. G., Galbraith, J. A., and Betzig, E. (2008) Live-cell photoactivated localization microscopy of nanoscale adhesion dynamics, *Nat. Meth.* **5**, 417–423.
67. Shroff, H., White, H., and Betzig, E. (2008) Photoactivated localization microscopy (PALM) of adhesion complexes, *Curr. Protoc. Cell Biol.* Juan S. Bonifacino, Ed. Chapter 4, Unit 4.21.
68. Vicente-Manzanares, M., Koach, M. A., Whitmore, L., Lamers, M. L., and Horwitz, A. F. (2008) Segregation and activation of myosin IIB creates a rear in migrating cells, *J. Cell Biol.* **183**, 543–554.
69. Liu, D., Bryceson, Y. T., Meckel, T., Vasiliver-Shamis, G., Dustin, M. L., and Long, E. O. (2009) Integrin-dependent organization and bidirectional vesicular traffic at cytotoxic immune synapses, *Immunity* **31**, 99–109.
70. Koster, A. J., and Klumperman, J. (2003) Electron microscopy in cell biology: integrating structure and function, *Nat. Rev. Mol. Cell Biol.* **Suppl**, SS6–10.
71. Hell, S. W. (2007) Far-field optical nanoscopy, *Science* **316**, 1153–1158.
72. de Lange, F., Cambi, A., Huijbens, R., de Bakker, B., Rensen, W., Garcia-Parajo, M., van Hulst, N., and Figdor, C. G. (2001) Cell biology beyond the diffraction limit: near-field scanning optical microscopy, *J. Cell Sci.* **114**, 4153–4160.
73. van Zanten, T. S., Cambi, A., Koopman, M., Joosten, B., Figdor, C. G., and Garcia-Parajo, M. F. (2009) Hotspots of GPI-anchored proteins and integrin nanoclusters function as nucleation sites for cell adhesion, *Proc. Natl. Acad. Sci. USA.* **106**, 18557–18562.
74. Henriques, R., and Mhlanga, M. M. (2009) PALM and STORM: what hides beyond the Rayleigh limit?, *Biotechnol. J.* **4**, 846–857.
75. Betzig, E., Patterson, G. H., Sougrat, R., Lindwasser, O. W., Olenych, S., Bonifacino, J. S., Davidson, M. W., Lippincott-Schwartz, J., and Hess, H. F. (2006) Imaging intracellular fluorescent proteins at nanometer resolution, *Science* **313**, 1642–1645.
76. Rust, M. J., Bates, M., and Zhuang, X. (2006) Sub-diffraction-limit imaging by stochastic optical reconstruction microscopy (STORM), *Nat. Meth.* **3**, 793–795.
77. Wang, Y., and Chien, S. (2007) Analysis of integrin signaling by fluorescence resonance energy transfer, *Meth. Enzymol.* **426**, 177–201.
78. Periasamy, A. (2001) Fluorescence resonance energy transfer microscopy: a mini review, *J. Biomed. Opt.* **6**, 287–291.
79. Buensuceso, C., De Virgilio, M., and Shattil, S. J. (2003) Detection of integrin α IIB β 3 clustering in living cells, *J. Biol. Chem.* **278**, 15217–15224.
80. Vararattanavech, A., Tang, M. L., Li, H. Y., Wong, C. H., Law, S. K., Torres, J., and Tan, S. M. (2008) Permissive transmembrane helix heterodimerization is required for the expression of a functional integrin, *Biochem. J.* **410**, 495–502.
81. Fu, G., Yang, H. Y., Wang, C., Zhang, F., You, Z. D., Wang, G. Y., He, C., Chen, Y. Z., and Xu, Z. Z. (2006) Detection of constitutive heterodimerization of the integrin Mac-1 subunits by fluorescence resonance energy transfer in living cells, *Biochem. Biophys. Res. Commun.* **346**, 986–991.
82. Tang, M. L., Vararattanavech, A., and Tan, S. M. (2008) Urokinase-type plasminogen activator receptor induces conformational changes in the integrin α M β 2 head-piece and reorientation of its transmembrane domains, *J. Biol. Chem.* **283**, 25392–25403.
83. Chigaev, A., Waller, A., Amit, O., and Sklar, L. A. (2008) α 4 β 1-integrin affinity: a possible mechanism for cell de-adhesion, *BMC Immunol.* **9**, 26.
84. Coutinho, A., Garcia, C., Gonzalez-Rodriguez, J., and Lillo, M. P. (2007) Conformational changes in human integrin α IIB β 3 after platelet activation, monitored by FRET, *Biophys. Chem.* **130**, 76–87.
85. Kim, M., Carman, C. V., Yang, W., Salas, A., and Springer, T. A. (2004) The primacy of affinity over clustering in regulation of adhesiveness of the integrin $\{\alpha\}L\{\beta\}2$, *J. Cell Biol.* **167**, 1241–1253.
86. Smith, E. A., Bunch, T. A., and Brower, D. L. (2007) General in vivo assay for the study of integrin cell membrane receptor microclustering, *Anal. Chem.* **79**, 3142–3147.
87. Deakin, N. O., Bass, M. D., Warwood, S., Schoelermann, J., Mostafavi-Pour, Z., Knight, D., Ballestrem, C., and Humphries, M. J. (2009) An integrin- α 4-14-3-3zeta-paxillin ternary complex mediates localised Cdc42 activity and accelerates cell migration, *J. Cell Sci.* **122**, 1654–1664.

88. Mocanu, M. M., Fazekas, Z., Petras, M., Nagy, P., Sebestyen, Z., Isola, J., Timar, J., Park, J. W., Vereb, G., and Szollosi, J. (2005) Associations of ErbB2, beta1-integrin and lipid rafts on Herceptin (Trastuzumab) resistant and sensitive tumor cell lines, *Cancer Lett.* **227**, 201–212.
89. Ng, T., Shima, D., Squire, A., Bastiaens, P. L., Gschmeissner, S., Humphries, M. J., and Parker, P. J. (1999) PKCalpha regulates beta1 integrin-dependent cell motility through association and control of integrin traffic, *EMBO J.* **18**, 3909–3923.
90. Parsons, M., Messert, A. J., Humphries, J. D., Deakin, N. O., and Humphries, M. J. (2008) Quantification of integrin receptor agonism by fluorescence lifetime imaging, *J. Cell Sci.* **121**, 265–271.
91. Stroeken, P. J., Alvarez, B., Van Rheenen, J., Wijnands, Y. M., Geerts, D., Jalink, K., and Roos, E. (2006) Integrin cytoplasmic domain-associated protein-1 (ICAP-1) interacts with the ROCK-I kinase at the plasma membrane, *J. Cell. Physiol.* **208**, 620–628.
92. Vielreicher, M., Harms, G., Butt, E., Walter, U., and Obergfell, A. (2007) Dynamic interaction between Src and C-terminal Src kinase in integrin alpha1Ib beta3-mediated signaling to the cytoskeleton, *J. Biol. Chem.* **282**, 33623–33631.
93. Lele, T. P., Thodeti, C. K., and Ingber, D. E. (2006) Force meets chemistry: analysis of mechanochemical conversion in focal adhesions using fluorescence recovery after photobleaching, *J. Cell. Biochem.* **97**, 1175–1183.
94. Chown, M. G., and Kumar, S. (2007) Imaging and manipulating the structural machinery of living cells on the micro- and nanoscale, *Int. J. Nanomed.* **2**, 333–344.
95. Hu, K., Ji, L., Applegate, K. T., Danuser, G., and Waterman-Storer, C. M. (2007) Differential transmission of actin motion within focal adhesions, *Science* **315**, 111–115.
96. Bulina, M. E., Lukyanov, K. A., Britanova, O. V., Onichtchouk, D., Lukyanov, S., and Chudakov, D. M. (2006) Chromophore-assisted light inactivation (CALI) using the phototoxic fluorescent protein KillerRed, *Nat. Protoc.* **1**, 947–953.
97. Rajfur, Z., Roy, P., Otey, C., Romer, L., and Jacobson, K. (2002) Dissecting the link between stress fibres and focal adhesions by CALI with EGFP fusion proteins, *Nat. Cell Biol.* **4**, 286–293.
98. Alon, R., and Dustin, M. L. (2007) Force as a Facilitator of Integrin Conformational Changes during Leukocyte Arrest on Blood Vessels and Antigen-Presenting Cells, *Immunity* **26**, 17–27.
99. Wang, N., Tytell, J. D., and Ingber, D. E. (2009) Mechanotransduction at a distance: mechanically coupling the extracellular matrix with the nucleus, *Nat. Rev. Mol. Cell Biol.* **10**, 75–82.
100. Puklin-Faucher, E., and Sheetz, M. P. (2009) The mechanical integrin cycle, *J. Cell Sci.* **122**, 179–186.
101. Cai, Y., and Sheetz, M. P. (2009) Force propagation across cells: mechanical coherence of dynamic cytoskeletons, *Curr. Opin. Cell Biol.* **21**, 47–50.
102. Sabouri-Ghomi, M., Wu, Y., Hahn, K., and Danuser, G. (2008) Visualizing and quantifying adhesive signals, *Curr. Opin. Cell Biol.* **20**, 541–550.
103. Wang, Y., Botvinick, E. L., Zhao, Y., Berns, M. W., Usami, S., Tsien, R. Y., and Chien, S. (2005) Visualizing the mechanical activation of Src, *Nature* **434**, 1040–1045.
104. Na, S., and Wang, N. (2008) Application of Fluorescence Resonance Energy Transfer and Magnetic Twisting Cytometry to Quantitate Mechano-Chemical Signaling Activities in a Living Cell, *Sci Signal* **26**, pl1.
105. Na, S., Collin, O., Chowdhury, F., Tay, B., Ouyang, M., Wang, Y., and Wang, N. (2008) Rapid signal transduction in living cells is a unique feature of mechanotransduction, *Proc. Natl. Acad. Sci. USA.* **105**, 6626–6631.
106. Goldyn, A. M., Rioja, B. A., Spatz, J. P., Ballestrem, C., and Kemkemer, R. (2009) Force-induced cell polarisation is linked to RhoA-driven microtubule-independent focal-adhesion sliding, *J. Cell Sci.* **122**, 3644–3651.
107. Brown, C. M., Hebert, B., Kolin, D. L., Zareno, J., Whitmore, L., Horwitz, A. R., and Wiseman, P. W. (2006) Probing the integrin-actin linkage using high-resolution protein velocity mapping, *J. Cell Sci.* **119**, 5204–5214.
108. Sabass, B., Gardel, M. L., Waterman, C. M., and Schwarz, U. S. (2008) High resolution traction force microscopy based on experimental and computational advances, *Biophys. J.* **94**, 207–220.
109. Gardel, M. L., Sabass, B., Ji, L., Danuser, G., Schwarz, U. S., and Waterman, C. M. (2008) Traction stress in focal adhesions correlates biphasically with actin retrograde flow speed, *J. Cell Biol.* **183**, 999–1005.